Dwarf Galaxies: From the Deep Universe to the Present
Proceedings IAU Symposium No. 344, 2019
K. B. W. McQuinn & S. Stierwalt, eds.

doi:10.1017/S1743921318005847

Atlas of Hα images for five hundred nearest dwarf galaxies

Serafim S. Kaisin and Igor D. Karachentsev

Special Astrophysical Observatory of the Russian Academy of Sciences, Nizhnij Arkhyz, Zelenchukskiy region, Karachai-Cherkessian Republic, Russia
emails: skai@sao.ru, ikar@sao.ru

Abstract. Results of mass imaging nearby dwarf galaxies in emission Hα line and red continuum with the 6-meter BTA telescope are available via the address: http://www.sao.ru/lv/lvgdb. The sample of dwarfs limited by a distance of 11 Mpc contains about 500 objects. Their Hα - fluxes are used to derive integrated and specific star formation rates of the galaxies. We evaluate the consistency between star formation rates obtained from our Hα-survey and GALEX far-ultraviolet survey. We fix a systematic rise of the ratio SFR(FUV)/SFR(Hα) with the decreasing stellar mass of dwarf galaxies. In the sample there were included only galaxies of late types: T = 10 (Ir), 9 (Im, BCD), 8 (Sdm), 7 (Sd), 6 (Scd), since elliptical and lenticular galaxies, and also spiral with massive bulges, have a significantly different history of star formation.

Keywords. Galaxies: dwarf, evolution, astronomical data bases: surveys, catalogs, stars: formation.

1. Introduction

Over the last years, the 6-meter BTA telescope of the Special Astrophysical Observatory has been used to image in the Balmer Hα line about 300 galaxies of the Local Volume (LV) with distances $D < 11$ Mpc. Images of some galaxies have been observed by us are presented in Fig. 1. The results of our observations are published in a series of papers seen below in the references.

Also a several surveys of nearby galaxies in the Hα emission line was published recently by Gil de Paz, *et al.* (2003), Hunter & Elmegreen (2004), James *et al.* (2004), Epinat *et al.* 2008, Meurer *et al.* (2006), and Bouchard *et al.* (2009). The most systematic observations in the Hα line were performed by Kennicutt *et al.* (2008). In summary, at the current time, the total number of the LV galaxies with measured Hα fluxes exceeded 500 objects. For the most of the galaxies far-ultraviolet fluxes (FUV) were measured also with the GALEX space telescope. Comparison the Hα and FUV fluxes gives an opportunity to identify burst and fade episodes of the star formation history occurring in dwarf galaxies on the time scales of $\sim 10 - 100$ million years.

2. Overview

As noted by Ricciardelli *et al.* (2015), and Karachentsev *et al.* (2018), the star formation rate (SFR) in late-type galaxies only little depends on the density of their environment. In other words, the rate of star formation in galaxies is determined mainly by their own individual properties, then by a tidal influence of the neighbors. The distribution of 506 LV galaxies in terms of the ratio of SFR measured via Hα and FUV fluxes is shown below in the Fig. 2 and 3.

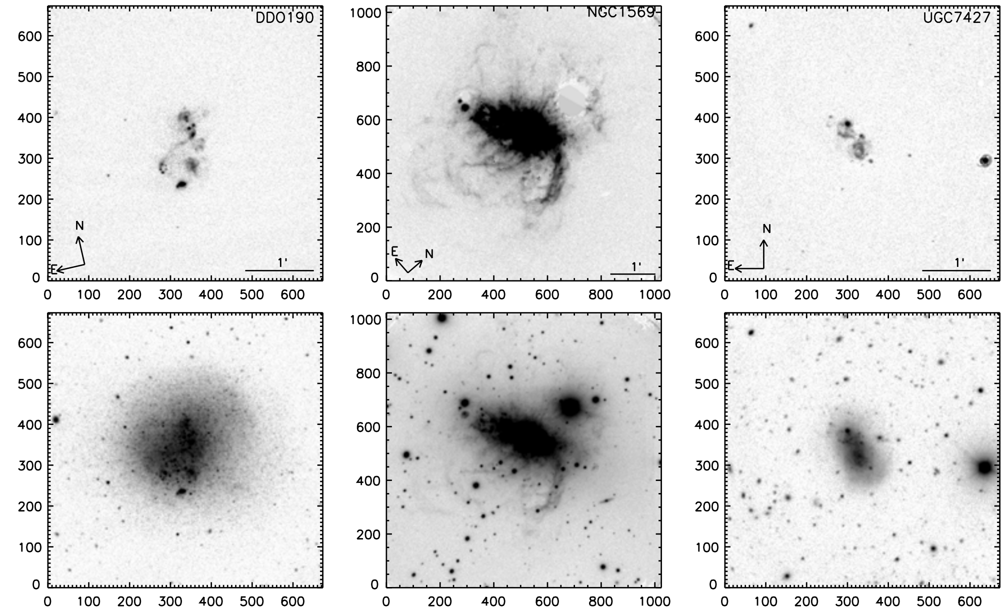

Figure 1. The bottom images in each pair represent the total exposure in the Hα line and in the continuum, and the top row images correspond to the "Hα - continuum" difference

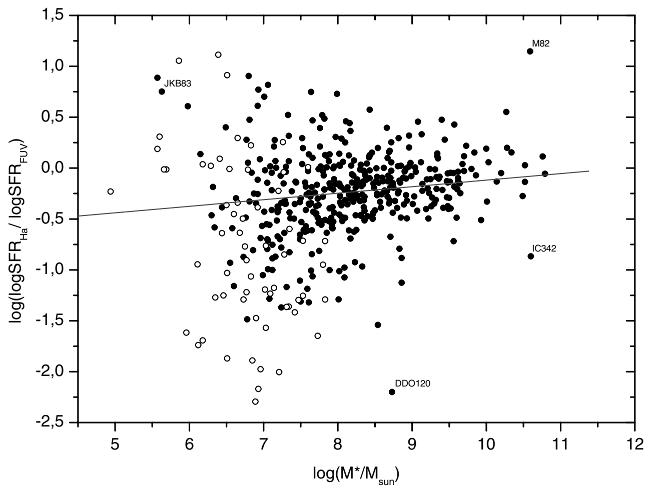

Figure 2. Ratio of Hα-to-FUV SFR vs. total stellar mass. Galaxies with measured FUV fluxes, but with the upper limit of the flux in Hα, are marked by empty circles.

As it is well known, the integral star-formation rate closely correlates with the luminosity or mass of a galaxy. Therefore, to characterize the process of star formation, the so-called specific star formation rate is usually used, sSFR = SFR/M* per unit of stellar mass. Along with this, the parameter SFE = SFR/MHI showing how quickly the available gas reserves in a galaxy will be used. Since both the stellar and gas masses of a galaxy are changing during the evolution, in the evolutionary picture without any

https://doi.org/10.1017/S1743921318005847 Published online by Cambridge University Press

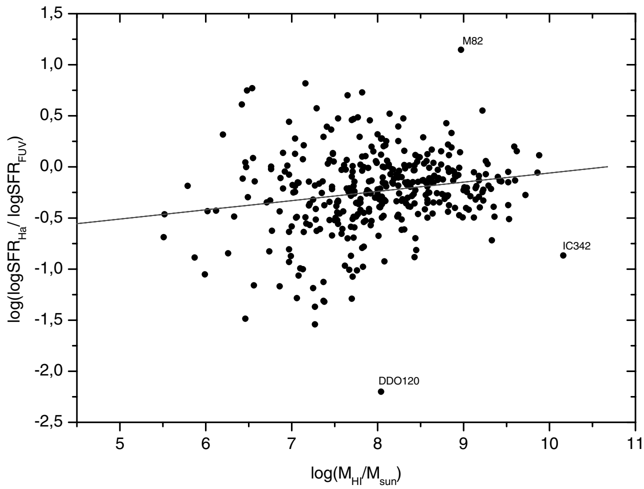

Figure 3. Ratio of Hα-to-FUV SFR vs. total hydrogen mass.

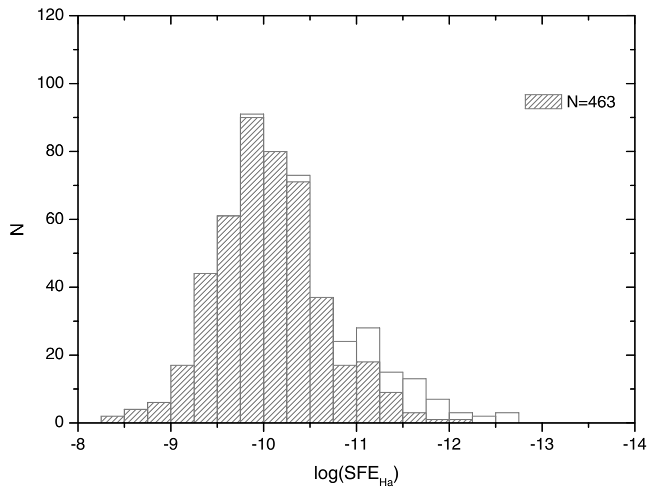

Figure 4. Distribution of LV galaxies from star-formation efficiency determined from Hα flux.

external influence, in the so-called "closed box", it is reasonable to introduce a new characteristic: the specific rate of star formation per unit of the baryon mass of a galaxy, bSFR = SFR/(M* + 1.85*MHI). Here, the factor 1.85 takes into account the contribution of helium and molecular hydrogen to the total mass of gas. Distribution of a number of LV galaxies in terms of the parameters: sSFR, SFE, and bSFR is presented in the Fig. 4, Fig. 5, Fig. 6 and Fig. 7. In each case, SFR was determined from the measured Hα fluxes. Galaxies with an upper limit of the Hα fluxes are shown without shading. Fig. 7 corresponds to bSFR values calculated from the FUV fluxes.

The data presented above allow to state that the processes of star formation in irregular dwarf galaxies and disks of spiral galaxies of late types have many similarities. Most of

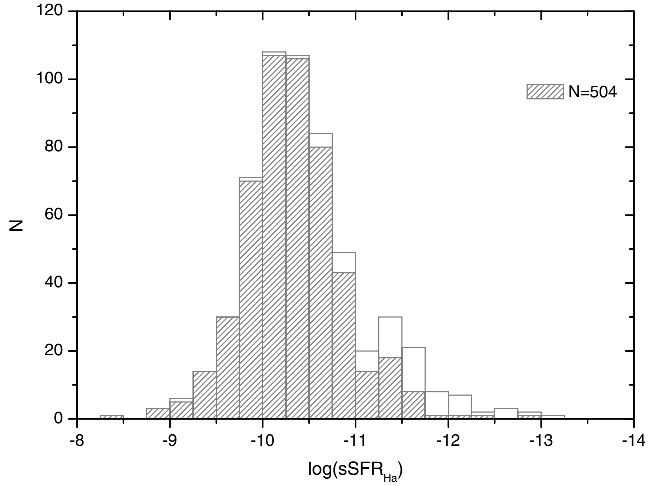

Figure 5. Distribution of LV galaxies from specific star-formation rate determined from Hα flux.

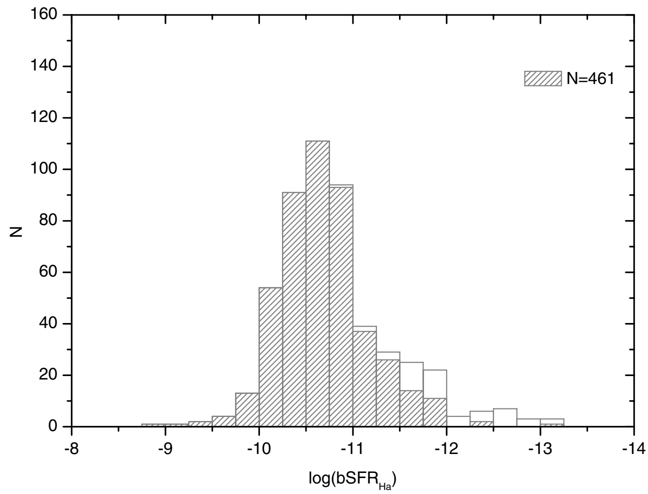

Figure 6. Distribution of LV galaxies from specific star-formation rate per unit baryonic mass of the galaxy determined from Hα flux.

the Scd-Sc-Sdm galaxies without visible bulge did not have probably merging events for the last ~ 10 Gyr. Such galaxies are characterized by a slow star formation rate. Dwarf irregular galaxies have roughly the same average specific star formation rate. However, as lower the baryon mass of the dwarf galaxy, as higher its SFR variations. The variations of star formation rate in the late-type galaxies are determined, basically, by individual parameters of these galaxies, being only little dependand on external influences.

Acknowledgements

This work was performed under support of the Russian Science Foundation grant 14-12-00965.

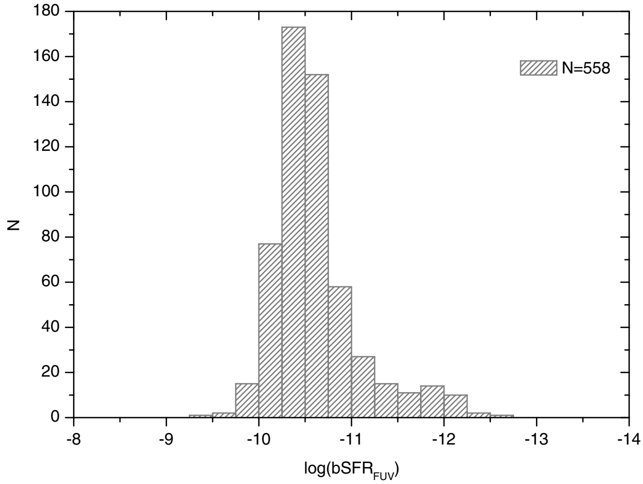

Figure 7. Distribution of LV galaxies from specific star-formation rate per unit baryonic mass of the galaxy determined from FUV measurements.

References

Bouchard A., Da Costa G. S., & Jerjen H. 2009, *AJ*, 137, 3038
Epinat B., Amram P., & Marcelin M. 2008, *MNRAS*, 390, 466
Kaisin S. S., & Karachentsev I. D. 2003, *ApJS*, 147, 29
Hunter D. A., & Elmegreen B. G. 2004, *AJ*, 128, 2170
James P. A., Shane N. S., & Beckman J. E. *et al.* 2004, *A&A*, 414, 23
Kaisin S. S., Kasparova A. V, Knyazev A. Yu., & Karachentsev I. D. 2007, *AstL*, 33, 283
Kaisin S. S., & Karachentsev I. D. 2008, *A&A*, 479, 603
Kaisin S. S., Karachentsev, I. D., & Kaisina E. I. 2011, *Ap*, 54, 315
Kaisin S. S., Karachentsev, I. D., & Ravindranath S. 2012, *MNRAS*, 425, 2083
Kaisin S. S., & Karachentsev I. D. 2013, *Ap*, 56, 305
Kaisin S. S., & Karachentsev I. D. 2013, *AstBu*, 68, 381
Kaisin S. S., & Karachentsev I. D. 2014, *AstBu*, 69. 390
Kaisin S. S., & Karachentsev I. D. 2018, *AstBu*, in press
Kaisin S. S., & Karachentsev I. D. 2006, *Ap*, 49, 287
Karachentsev I. D., & Kaisin S. S. 2007, *AJ*, 133, 1883
Karachentsev I. D., & Kaisin S. S. 2010, *AJ*, 140, 1241
Karachentsev I. D. Kaisin S. S., & Kaisina E. I. 2015, *Ap*, 33, 58, 453
Karachentsev I. D., Kaisina E. I., & Makarov D. I., 2018, *MNRAS*, 480, 1697
Kennicutt R. C., Lee J. C., & Funes J. G. *et al.* 2008, *ApJS*, 178, 247
Meurer G. R., Hanish D. J., & Ferguson H. C. *et al.* 2006, *ApJS*, 165, 307
Ricciardelli E., Cava A., Varela J., & Quilis V. 2015, *MNRAS*, 445, 4045